γ-ray spectroscopy of ^{42}K and ^{43}K

M. Moralles,* P. Jänker, H. Leitz, K. E. G. Löbner, K. Rudolph, F. J. Schindler, H.-G. Thies, and T. Winkelmann
Sektion Physik, Universität München, Am Coulombwall 1, D-85748 Garching, Germany

P. R. Pascholati
Instituto de Física da Universidade de São Paulo, CP 66318, CEP 05315-970 São Paulo, SP, Brazil

B. A. Brown
National Superconducting Cyclotron Laboratory and Department of Physics, Michigan State University, East Lansing, Michigan 48824
(Received 9 April 1998)

Excited states of ^{42}K and ^{43}K were investigated using the reactions ^{9}Be(^{36}S,$2np$)^{42}K and ^{9}Be(^{36}S,np)^{43}K. Three methods of selective γ-ray spectroscopy were employed: recoil-nuclei-γ, proton-γ, and γ-γ coincidence measurements. Thirty-eight electromagnetic transitions were observed originally, 22 belonging to ^{42}K and 16 belonging to ^{43}K. Eight new levels are suggested for ^{42}K and four for ^{43}K. Shell-model calculations were performed in the $(sd)^{-1}(fp)^{3}$ space to obtain negative-parity states of ^{42}K and $(sd)^{-1}(fp)^{4}$ space for positive-parity states of ^{43}K. The calculated energies are in good agreement with the experimental values, but some systematic differences indicate that the collectivity of the actual levels is not completely accounted for by the configuration space used in the calculations. [S0556-2813(98)01408-3]

PACS number(s): 23.20.Lv, 25.70.Gh, 27.40.+z, 29.30.Aj

I. INTRODUCTION

High-spin states of nuclei in the $A \approx 40$ mass region have been the subject of many studies in the last three decades. The interest in this region began to increase in the 1960s with the observation of deformed states in the doubly magic ^{40}Ca [1,2]. After that, spectroscopy of ^{42,43,44}Ca [3–5] and ^{38,40}Ar [6,7] revealed also deformed states at low-excitation energies, indicating that nuclei near the closed shells with Z or $N=20$ can easily lose the spherical shape. On the other hand, results of experiments that searched for deformations in other nuclei, like ^{44}Sc and ^{44}Ti [8], did not show high-spin states with rotational features.

Recently, the employment of sophisticated techniques of γ spectroscopy permitted the observation of high-spin states of ^{40}Cl [9], ^{47}Ti, ^{47,48}V, and ^{47,48}Cr [10,11]. The results of ^{40}Cl showed that negative-parity yrast states up to $J^{\pi}=8^{-}$ are well explained by shell-model calculations, while the Ti, V, and Cr isotopes presented states with features of permanent deformation coexisting with states of pure shell-model characteristics, like band termination and cross-conjugate symmetry.

These and other results of investigations in this mass region indicate that a systematic understanding of the interplay between single-particle and collective states involving nucleons in the $2s-1d$ and $1f-2p$ shells is not well established. Therefore, it is important to study nuclei with many different combinations of proton and neutron numbers in these shells. Compared to other nuclides in this region, little is known about the high-spin states of neutron-rich potassium isotopes. The main reason is the difficulty in accessing them through the fusion-evaporation reactions of stable nuclei, which is the most common way to produce excited nuclei with large values of angular momenta.

Most of the known excited states of ^{42}K were determined through neutron capture and neutron transfer reactions [12]. These experiments revealed a large number of low-spin states, since such reactions do not transfer much angular momentum. The known levels with highest spins were observed through γ-ray spectroscopy of the fusion-evaporation reaction ^{26}Mg(^{18}O,pn)^{42}K [13,14]. The last compilation of experimental data of ^{42}K shows only three levels with spins higher than $4\hbar$ [15].

Behbehani *et al.* [16] investigated high-spin states of ^{43}K using the ^{40}Ar(α,p) reaction and established excited states with spins up to $15\hbar/2$. Recently Kozub *et al.* [17] reported results of γ-proton measurements using the ^{9}Be(^{36}S,np)^{43}K reaction. They included two new levels with probable spins of $13\hbar/2$ and $15\hbar/2$.

The present work reports the investigation of excited states of ^{42}K and ^{43}K produced in the ^{36}S $+^{9}$Be reaction using γ-ray spectroscopy. The description of the experimental methods, the obtained results, and a discussion of the level schemes are presented in the following sections.

II. EXPERIMENTAL PROCEDURE

The experiments were performed at the TANDEM accelerator of the University and Technical University Munich, using ^{36}S projectiles impinging on beryllium targets. Table I shows the predicted cross sections for the strongest reaction channels obtained from the code CASCADE [18] for beam energies of 90, 100, and 110 MeV. The use of filtering techniques for the observation of γ rays is essential in this case, since several evaporation channels are open and the produc-

*Author to whom correspondence should be addressed; Permanent address: Instituto de Pesquisas Energéticas e Nucleares, CP 11049, CEP 05422-970 São Paulo, SP, Brazil; Electronic address: moralles@curiango.ipen.br

TABLE I. Calculated cross sections (mb) for the strongest channels of the ^{9}Be(^{36}S,X)Y reaction at laboratory energies of 90, 100, and 110 MeV obtained from the simulation code CASCADE [18].

X	Y	90 MeV	100 MeV	110 MeV
$2n$	^{43}Ca	146	96	62
$3n$	^{42}Ca	287	301	290
np	^{43}K	56	42	31
$2np$	^{42}K	97	140	174
$n\alpha$	^{40}Ar	37	28	21
$2n\alpha$	^{39}Ar	180	244	311

tion of the K isotopes is small in comparison to some isotopes of Ca and Ar. Two experimental setups were used to perform three types of selective γ-ray spectroscopy, as described in the next subsections. In the first experiment, γ-ray spectra were measured in coincidence with the recoiling nuclei, allowing the unambiguous assignment of the γ rays to different isotopes. With the second setup, γ-charged-particle and γ-γ measurements were carried out, which provided results with more precise energies and coincidence relations.

A. Recoil-nuclei-γ coincidence experiment

Prompt γ-ray spectra were measured in coincidence with identified recoil nuclei (=evaporation residues) using the Munich high-frequency recoil spectrometer [19,20] equipped with an annular Compton-suppressed HPGe detector positioned at 180° relative to the beam direction. The energy resolution and relative efficiency at 1.3 MeV (^{60}Co) were approximately 2.8 keV and 25%, respectively. A scheme of the experimental arrangement is shown in Fig. 1. The pulsed ^{36}S beam ($E_{\rm lab}$=100 MeV) passes through the hole in the HPGe detector and reaches the beryllium target (150 μg/cm^2) at a speed of 2.3 cm/ns. Following the fusion reaction, the ^{45}Ca* compound nuclei emit neutrons, α particles, and protons, forming mainly ^{42}Ca, ^{39}Ar, ^{43}Ca, ^{42}K, ^{43}K, and ^{40}Ar with cross sections varying from approximately 300 to 30 mb (see Table I). The excited evaporation residues with velocities around 1.8 cm/ns decay mostly by prompt γ-ray emission near the target position and leave the reaction chamber at angles near 0°. Since the efficiency of the recoil spectrometer is largest at 0°, the kinematics of inverse reactions is preferable [20].

The evaporation residues are separated from the beam particles by using a velocity filter. The beam is deflected out of the 0° direction with a combination of a high-frequency electric field and the magnetic field of two dipole magnets (see Fig. 1). The evaporation residues are slower than the beam particles and reach the electric-field region later, when the electric field has changed the orientation, so they are deflected by the electric field in a way to compensate the magnetic deflection and leave the filter at 0°. The optimum condition for the elimination of the beam particles is achieved by choosing the right distance between the target and the high-frequency field, and by adjusting the phase of the high-frequency electric field relative to the pulsed beam (see Ref. [19] for more details).

The data were stored event by event on magnetic tapes and off-line analysis was carried out later. The atomic number Z of the evaporation residues is obtained from the energy loss and total-energy measurements in a three-sector ionization chamber. The time difference Δt, between the signal of a microchannel plate and the signal of the pulsed beam, permits the determination of the velocity of the residues. The mass number A is derived from the total energy and the velocity. Figure 2 shows the contour plot of a two-dimensional (A vs Z) matrix obtained for the evaporation residues of the ^{36}S +^{9}Be reaction. Unique identification of the evaporation residues is obtained with this system.

The energy calibration for the γ-ray spectra in coincidence with recoil nuclei was performed by using the following transitions: 106.828(7), 151.433(11), 440.82(3), and 676.88(10) keV from ^{42}K, 1112.0(4) keV from ^{43}K, 809.6(3), 1524.73(3), 2301.77(24), 2554.89(24), and 3219.34(24) keV from ^{42}Ca, and 372.762(7) keV from ^{43}Ca [15]. The relative efficiency at the target position was cali-

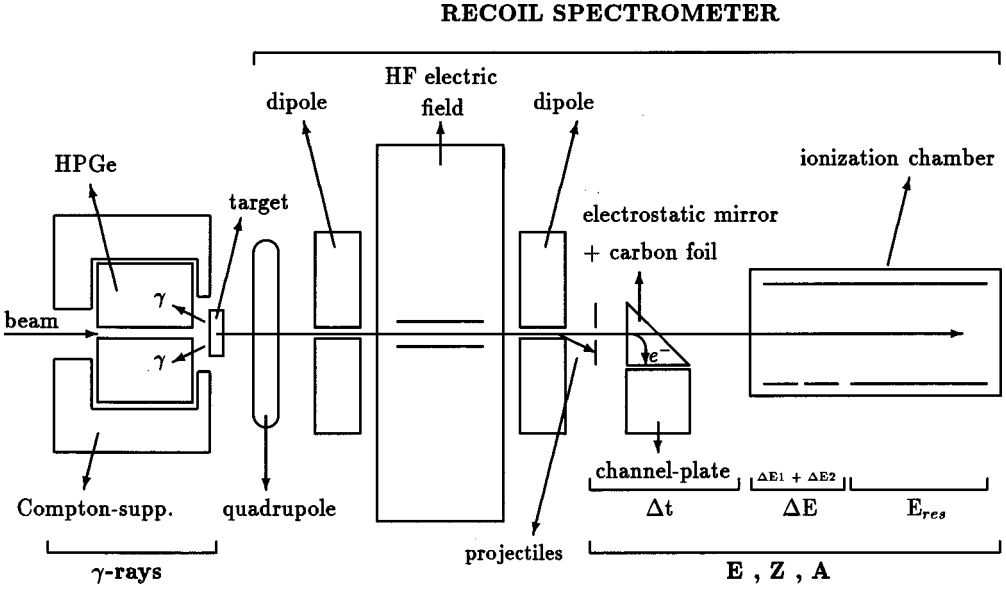

FIG. 1. Scheme of the setup used in the recoil-nuclei-γ measurements (see text for details).

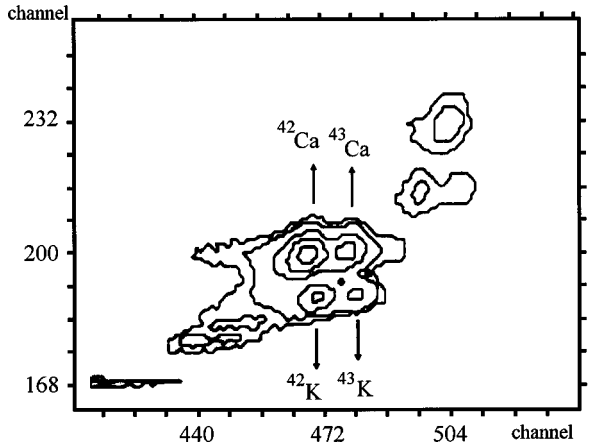

FIG. 2. A vs Z contour plot of recoil nuclei obtained with the Munich recoil spectrometer for the ^{36}S $+^{9}$Be reaction ($E_{\mathrm{lab}}=100$ MeV).

brated by using standard sources of ^{152}Eu, ^{133}Ba, and ^{60}Co for energies between 0.1 and 1.4 MeV. Known branching ratios [15] of γ transitions from ^{42}Ca (levels of 2424 and 5744 keV) and from ^{43}Ca (levels of 4395 and 4590 keV) provided calibration data for relative efficiency up to the energy of 2.7 MeV.

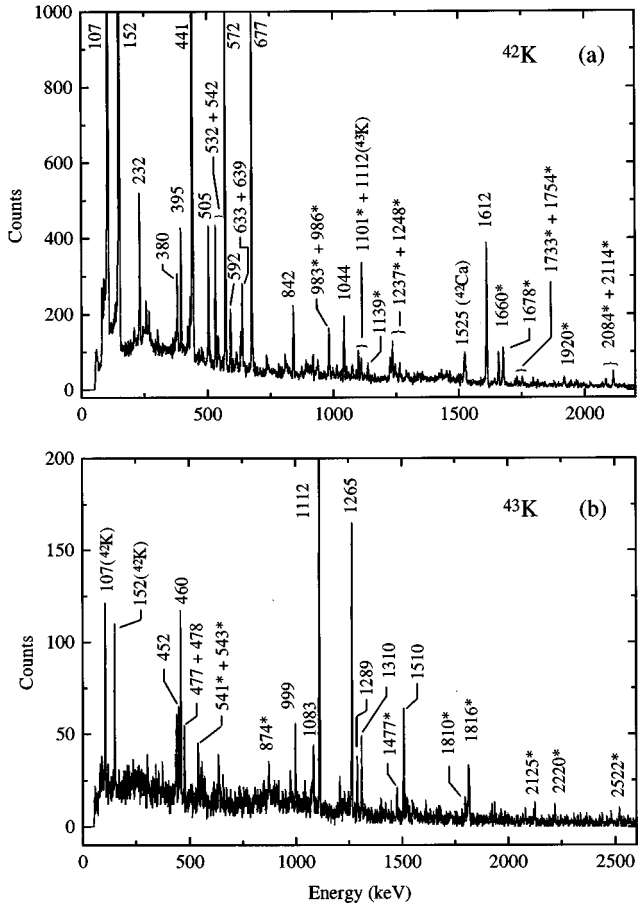

FIG. 3. γ-ray spectra in coincidence with ^{42}K (a) and with ^{43}K (b) recoils. γ-ray peaks marked with asterisks were observed in this work. The presence of peaks produced in other evaporation channels are identified with the respective nuclide.

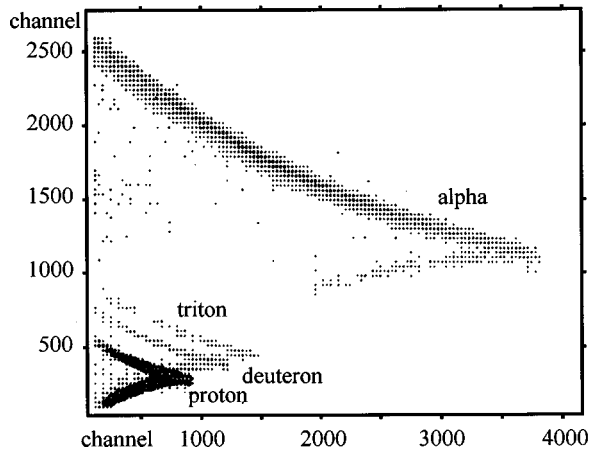

FIG. 4. Typical ΔE vs E_{residual} matrix as measured with one of the eleven telescopes in the forward direction.

Some considerations about the measured γ-ray energies and intensities should be mentioned, since the evaporation residues leave the target with approximately 6% of the speed of light. The energy values must be corrected for Doppler shift, which is performed off-line for each γ ray by using the velocity of the coincident nucleus. The intensity evaluations of the γ rays are subject to systematic errors, because the

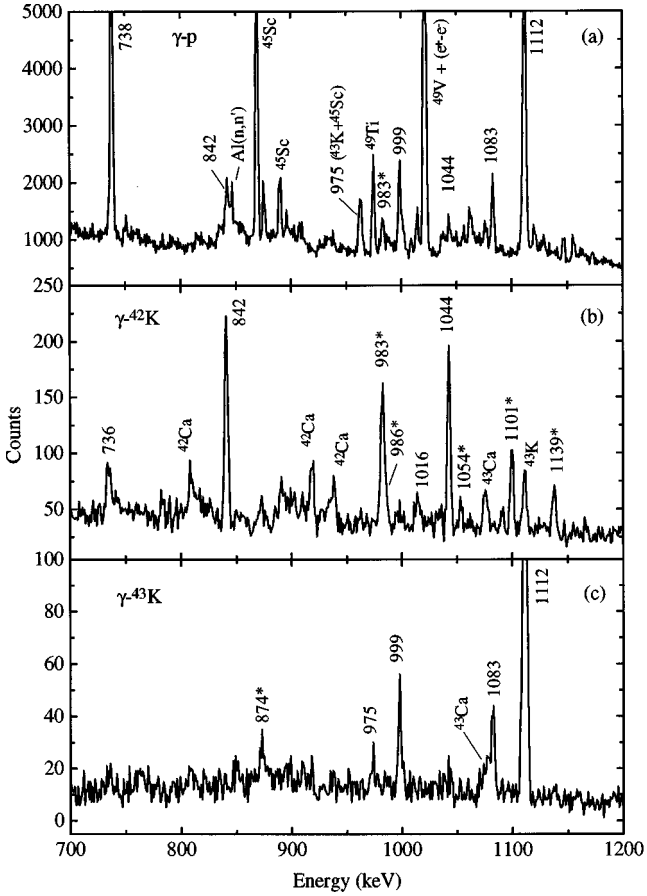

FIG. 5. γ-ray spectra of the energy range from 700 to 1200 keV in coincidence with protons (a), ^{42}K recoils (b), and ^{43}K recoils (c). γ-ray peaks marked with asterisks were observed in this work.

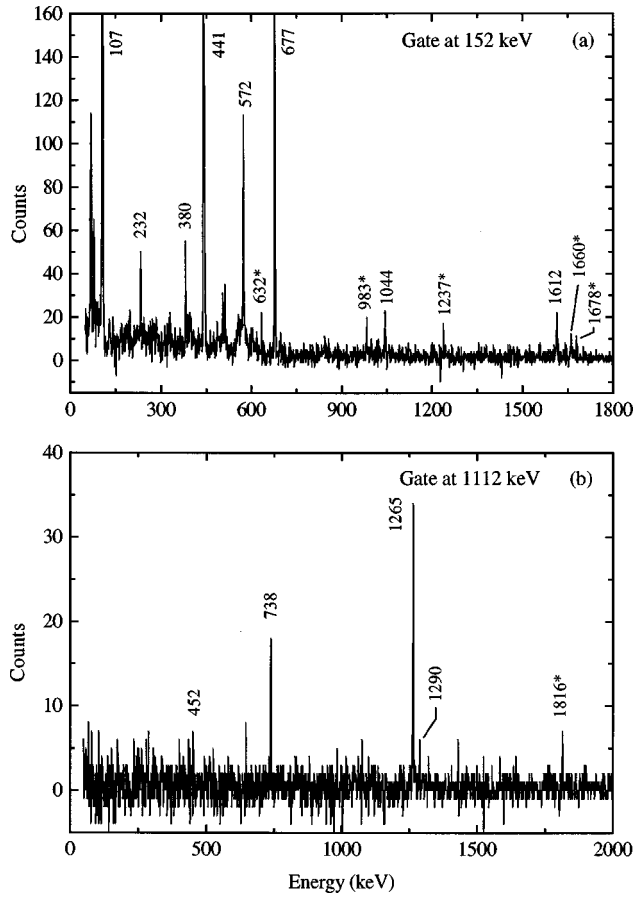

FIG. 6. γ-ray spectrum gated by 152 keV γ rays belonging to ^{42}K (a) and gated by 1112 keV γ rays belonging to ^{43}K (b). γ-ray peaks marked with asterisks were observed in this work.

γ-ray emission can occur far from the target position if the half-life of the decaying level is long ($T_{1/2} \gtrsim 10^{-9}$ s). Hence the presence of levels with long half-lives may make the intensity analysis inaccurate or even impracticable if the half-lives are unknown. As an example of the effect, the intensity of a γ transition from a level with a half-life of 1 ns is suppressed to approximately 61% relative to the intensity measured with nuclei at rest for prompt γ rays ($T_{1/2} < 100$ ps), considering a detection efficiency decreasing with the square of the distance from the detector.

Doppler-shift-corrected γ-ray spectra in coincidence with ^{42}K and ^{43}K ions are shown in Figs. 3(a) and 3(b), respectively. The main feature of these spectra is the almost total absence of peaks from evaporation channels other than those from the selected one. Spurious transitions, like the ones indicated with ^{42}Ca in the ^{42}K spectrum and with ^{42}K in the ^{43}K spectrum, are easily identified.

B. Charged-particle-γ and γ-γ coincidence experiments

The charged-particle-γ and γ-γ coincidence experiments were carried out with 95 MeV ^{36}S projectiles on a 610 μg/cm^2 beryllium target evaporated on a 36 mg/cm^2 gold backing. The target was positioned at the center of a spherical aluminum chamber (radius=12 cm) surrounded by five Compton-suppressed HPGe detectors on the equatorial plane at azimuthal angles of 36°, 72°, 118°, 235°, and 306°. The detector at 235° was the same used with the recoil spectrometer and the other four have typical relative efficiencies of 30% and energy resolution of 2.0 keV at 1.3 MeV; one of them (36°) suffered resolution deterioration during the experiment and its energy resolution was about 2.7 keV at the end of the measurements.

Particle detectors were installed in a very compact geometry at forward and backward angles, covering approximately 15% of the full solid angle. The gold backing was thick enough to stop both evaporation residues and beam particles, but allowed the passage of the light particles to be detected at forward angles.

Eleven telescopes consisting of two PIN-diodes were placed at forward angles. They were not thick enough to stop the most energetic evaporated particles, however they allowed the particle identification as illustrated in Fig. 4. The impossibility of obtaining the total energy of the particles did not affect the quality of the results, as one is interested only in the identification. Figure 4 demonstrates that it is always possible to choose a region that contains only one type of particle. Seven single PIN-diodes were used at backward angles because the reaction's kinematics permitted only $Z=1$ particles at those angles and the particle identification was not necessary. Gold foils with 25 mg/cm^2 were placed in front of the PIN-diodes to suppress the high intensity of backscattered beam particles.

The energy calibration for the γ spectra in coincidence with charged particles was performed by using the following transitions: 106.828(7) and 440.82(3) keV from ^{42}K, 250.332(11) and 2092.69(2) keV from ^{39}Ar, 646.170(10) keV from ^{37}S, 1460.830(5) keV from ^{40}Ar, 3103.36(2) keV from ^{37}Cl [15], 159.368(20) keV from ^{47}Ti [21], 889.276(3) and 1120.545(4) keV from ^{46}Ti [22]. The calibration curve of the relative efficiency at the target position was fitted from data obtained with standard sources of ^{152}Eu, ^{133}Ba, ^{60}Co, and ^{166m}Ho.

The data acquisition was carried out for three days with the coincidence requirement of at least one γ ray and one charged particle. For the γ-γ coincidence mode the total acquisition time was 8 h with beam energies of 95 MeV (4 h) and 130 MeV (4 h).

Only the spectra of the three detectors with good resolution were added to obtain a high statistics proton-gated γ spectrum, since the inclusion of the data from the two Ge detectors with worse energy resolution mentioned above diminished the quality of the summed spectrum. However, the two poor-resolution Ge detectors were used in the γ-γ analysis.

The presence of carbon and oxygen in the target was evidenced from the observation of characteristic γ rays of Ca and Ti isotopes in coincidence with α particles, and γ rays of Sc and V isotopes in coincidence with protons. Carbon and oxygen, even at small fractions, produce detectable amounts of evaporation residues because the reactions with the beam have large cross sections, as pointed out also in another work which used the same reaction [9].

Figures 5(a), 5(b), and 5(c) show the same energy region of the γ-ray spectra in coincidence with protons, ^{42}K, and ^{43}K recoils, respectively. The differences between data obtained in coincidence with recoil nuclei and with protons are very pronounced. The proton-gated γ-ray spectrum has high statistics and good resolution, but reveals the presence of

TABLE II. Energies, relative intensities, and assignments of the γ rays of ^{42}K.

Energy [a] (keV)	Relative intensity [b]	Transition $E_i \rightarrow E_f$	Energy [a] (keV)	Relative intensity [b]	Transition $E_i \rightarrow E_f$
106.83(5)	100.0(17)	107→0	986.1(4) [c d]	0.94(25) [e]	2525→1539
151.48(4)	103.5(20)	258→107	1015.5(4) [d]	0.91(25) [e]	1273→258
232.4(4)	5.95(24)	1376→1144	1043.79(14) [d]	2.74(25)	2992→1948
380.39(5)	3.93(15)	639→258	1054.3(3) [c d]	0.67(15) [e]	3168→2114
395.16(7)	3.55(19)	1539→1144	1100.67(18) [c d]	2.06(20) [e]	4092→2992
422.8(3) [c d]	2.3(3)	2359→1936	1138.78(24) [c d]	1.24(17) [e]	3498→2359
431.44(9)	1.73(26)	1273→842	1237.07(16) [c d]	2.80(24) [e]	1936→699
440.78(4)	77.4(11)	699→258	1248.00(27) [c d]	1.13(16) [e]	4746→3498
444.43(5)	5.12(26)	1144→699	1291.4(6) [c d]	0.45(13) [e]	Not assigned
504.83(4)	12.41(28)	1144→639	1296.6(6) [c d]	0.51(13) [e]	Not assigned
531.80(6)	8.8(5)	639→107	1511.2(5) [c d]	0.65(16) [e]	Not assigned
542.42(23) [c d]	5.59(25)	Not assigned	1612.19(11) [d]	2.55(26)	3560→1948
571.86(4)	7.7(23)	1948→1376	1659.91(16) [c]	1.78(24)	2359→699
592.23(6)	3.58(21)	699→107	1677.52(26) [c d]	2.3(5) [e]	1936→258
616.09(29) [d]	2.4(3)	1255→638	1682.9(5) [c d]	0.55(14) [e]	2525→842
632.68(20) [c d]	1.79(20)	2992 → 2359	1732.6(6) [c d]	0.74(22) [e]	4092→2359
638.60(5)	5.7(3)	639→0	1754.4 (3) [c d]	1.00(17) [e]	4746→2992
676.77(4)	47.8(7)	1376→699	1919.9(4) [c d]	0.73(20) [e]	Not assigned
682.09(11)	1.72(16)	682→0	2024.5(6) [c d]	0.41(11) [e]	3168→1144
735.7(3) [d]	0.79(14) [e]	Not assigned	2083.7(5) [c d]	0.71(14) [e]	2766→682
841.78(10)	4.7(4)	842→0	2113.8(3) [c d]	2.1(3) [e]	2114→0
983.16(9) [c]	4.7(5)	2359→1376			

[a]Obtained from the proton-γ coincidence spectra, unless otherwise indicated.
[b]Obtained from the sum of three spectra in coincidence with protons (E_{lab}=95 MeV), unless otherwise indicated. Uncertainties are statistical only.
[c]Observed for the first time in this work.
[d]Obtained from the recoil-gated γ-ray spectrum.
[e]Obtained from the recoil-gated γ-ray spectrum (E_{lab}=100 MeV); subject to systematic errors (see text for details).

contributions from contaminants and also from transitions produced by neutron scattering on the surrounding materials. The lower statistics and poor resolution of the recoil-gated γ-ray spectra is compensated with the minor spurious contributions. Another point to notice in these figures is the total absence of the strong 738 keV transition in coincidence with ^{43}K nuclei. This is a $M2(+E3)$ transition with a known half-life of 200 ns [15], which is too long to be detected (see Sec. II A). Figures 6(a) and 6(b) show γ-ray spectra gated by 152 keV (^{42}K) and 1112 keV (^{43}K) γ rays, respectively.

TABLE III. γ-γ coincidences of transitions belonging to ^{42}K.

Gate (keV)	γ rays in coincidence
107	152; 232; 380; 395; 441; 444; 505; 532; 572; 592; 616; 632; 677; 983; 1044; 1237; 1612; 1660; 1678
152	107; 232; 380; 395; 441; 444; 505; 572; 616; 632; 677; 983; 1044; 1237; 1612; 1660; 1678
441	107; 152; 232; 395; 444; 572; 632; 677; 983; 1044; 1237; 1612; 1660
572	107; 152; 232; 441; 505; 532; 677; 1044; 1612
677	107; 152; 441; 572; 592; 983; 1044; 1612
1237	107; 152; 441
1612	107; 152; 441; 572; 677
1678	107; 152

III. RESULTS AND LEVEL SCHEMES

The three experiments provided results with different characteristics and the analysis was performed taking into account the advantages of each one. Tables II and IV summarize the results obtained from the γ-ray spectra, and Tables III and V contain the γ-γ coincidence data. The uncertainties of the intensities correspond to the statistical contribution only; angular distribution was not taken into account. The fitting of the peaks was performed by using Gaussian shapes with fixed widths. The widths were chosen according to a calibration function obtained from well-shaped peaks with good statistics and free from Doppler shift. This procedure permits one to discard peaks which are affected by the Doppler effect in the γ spectra in coincidence with protons, because they have different widths and shapes. For such peaks the χ^2 values for the Gaussian fit with fixed widths are not acceptable.

The assignments of the γ rays to their respective nuclides were obtained by using only the data of the recoil-gated

TABLE IV. Energies, relative intensities, and assignments of the γ rays of ^{43}K.

Energy [a] (keV)	Relative intensity [b]	Transition $E_i \rightarrow E_f$	Energy [a] (keV)	Relative intensity [b]	Transition $E_i \rightarrow E_f$
303.10(5)	4.33(14)	1510→1207	1265.08(7)	33.9(18)	3116→1850
451.82(4)	7.7(3)	3592→3140	1289.54(7)	12.0(4)	3140→1850
459.91(4)	21.7(6)	2509→2049	1310.55(7)	26.1(7)	2049→738
476.59(6) [f]	5.38(24)	1987→1510	1401.0(5) [c d]	1.2(3) [e]	4541→3140
478.48(11)	2.20(20)	2987→2509	1477.0(3) [c d]	5.9(12) [e]	3986→2509
540.7(4) [c d]	4.6(13) [e]	Not assigned	1510.00(10)	37.3(22)	1510→0
543.1(5) [c d]	4.0(13) [e]	Not assigned	1553.1(6) [c d]	1.3(3) [e]	4541→2987
555.2(3) [c d]	1.4(3) [e]	4541→3986	1798.5(4) [c d]	4.5(12) [e]	Not assigned
561.09(5)	8.30(25)	561→0	1810.0(6) [c d]	4.5(13) [e]	Not assigned
738.26(5)	>62 [g]	738→0	1815.61(26) [c d]	18.3(27) [e]	4931→3116
873.9(4) [c d]	4.1(10) [e]	2081→1207	1936.4(5) [c d]	3.8(10) [e]	3986→2049
975.06(5)	8.1(25)	975→0	2081.3(7) [c d]	2.7(9) [e]	2081→0
998.84(6)	13.9(6)	2509→1510	2124.9(4) [c d]	7.0(14) [e]	Not assigned
1083.19(6)	11.8(4)	3592→2509	2219.8(6) [c d]	4.0(10) [e]	Not assigned
1110.04(12)	9.0(11)	1110→0	2442.3(6) [c d]	2.9(10) [e]	Not assigned
1112.17(6)	100.0(22)	1850→738	2521.6(5) [c d]	4.3(11) [e]	Not assigned
1206.94(7)	13.6(4)	1207→0			

[a]Obtained from the proton-γ coincidence spectra, unless otherwise indicated.

[b]Obtained from the sum of three spectra in coincidence with protons (E_{lab}=95 MeV), unless otherwise indicated. Uncertainties are statistical only.

[c]Observed for the first time in this work.

[d]Obtained from the recoil-gated γ-ray spectrum.

[e]Obtained from the recoil-gated γ-ray spectrum (E_{lab}=100 MeV); subject to systematic errors (see text for details).

[f]This γ ray is interpreted as a doublet in Ref. [17]; our data do not permit us to resolve it.

[g]Transition from a long-lived state ($T_{1/2}$=200 ns); part of the events were outside of the coincidence window.

γ-ray spectra. Two exceptions were the 738 keV line (see Fig. 5 and explanation in the previous section) and the weak 1110 keV transition, which could not be separated from the strong 1112 keV line due to the insufficient energy resolution of the Ge detector used with the recoil spectrometer.

The relative intensities, listed in the second and fifth columns of Tables II and IV, were obtained from the sum of the proton-γ coincidence data using the γ-ray spectra of the three Ge detectors with best energy resolution. Intensities measured in coincidence with recoil nuclei are indicated.

The construction of the level schemes was performed by applying a procedure that takes into account the different types of information obtained in the three experiments. This procedure started with the known levels and the new γ rays to establish new levels, as described below.

(a) A new level with energy E_i was determined by searching for values that satisfy the following condition:

TABLE V. γ-γ coincidences of transitions belonging to ^{43}K.

Gate (keV)	γ-rays in coincidence
738	460; 1112; 1311
1112	452; 738; 1265; 1290; 1816
1265	738; 1112
1290	452
1510	999

$$||E_i - E_f| - T_j| \leqslant (\Delta E_f^2 + \Delta T_j^2)^{1/2}, \quad (1)$$

where E_f (ΔE_f) and T_j (ΔT_j) are the energies (uncertainties) of the known levels and new transitions, respectively. The known levels of ^{42}K and ^{43}K are taken from the compilation of Endt [15]. A level was considered as a candidate if condition (1) was satisfied for at least two combinations of new transitions and known levels. This procedure is in part similar to that described by Helmer and Bäcklin [23], but the statistical analysis developed by those authors is not applicable for the present treatment.

(b) Consistency of the intensities was verified, i.e., the intensity feeding a level cannot be larger than the depopulating intensity.

(c) Spin compatibility was verified if any information about the spins of the known levels was available. Transitions with multipolarities larger than two were discarded and the competition between transitions that depopulate the same level should have compatible transition probabilities.

(d) Consistency with the γ-γ coincidences was verified.

(e) When the four conditions above were satisfied, a least-squares fit of the level scheme was carried out using the method described by Vanin *et al.* [24], including the supposed new level. The χ^2 value of the fit and the absolute residue of each new transition were used to decide on the acceptance of the new level.

(f) When a new level was accepted, it was taken as a

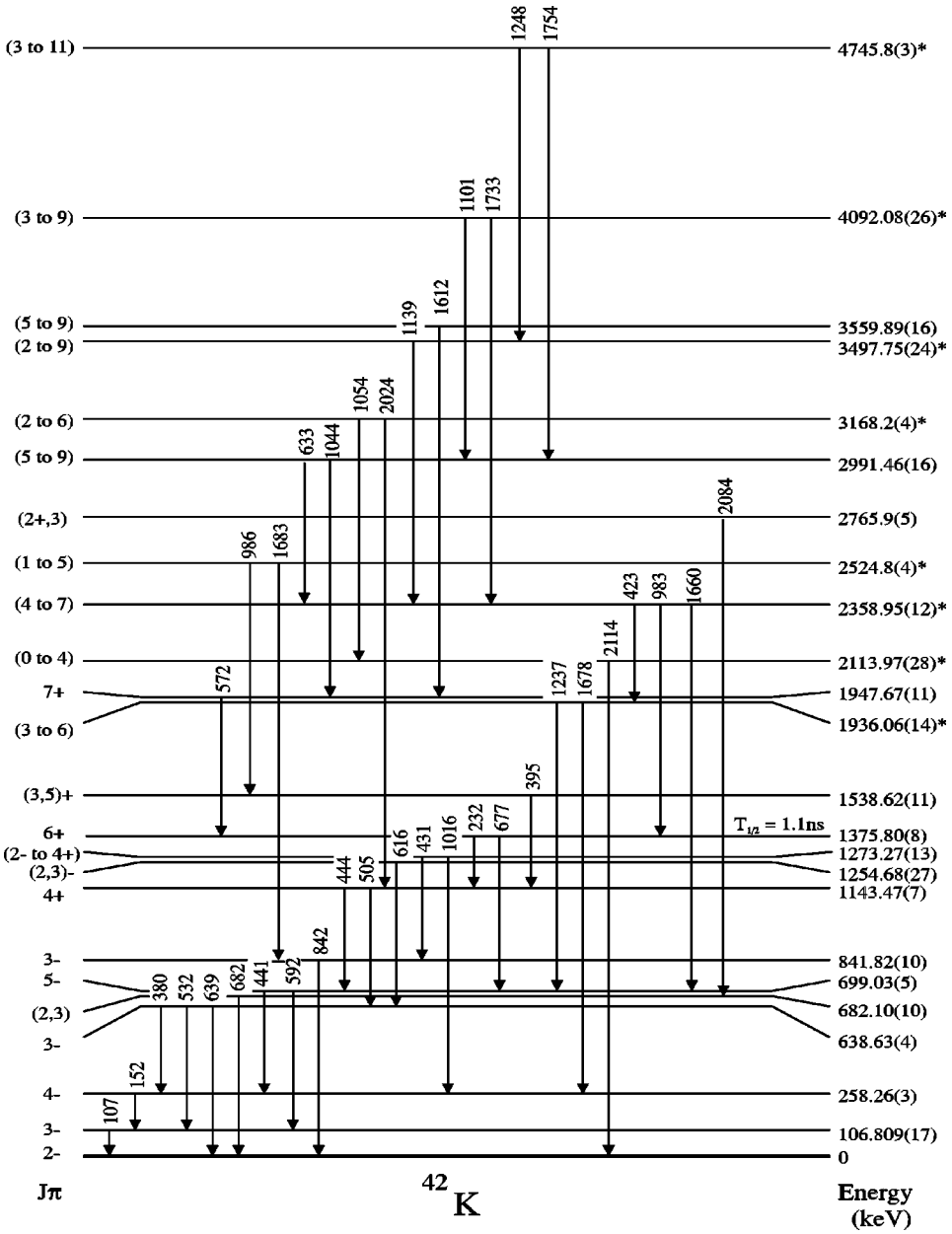

FIG. 7. Level scheme of ^{42}K proposed in this work. New suggested levels are indicated with asterisks. Spin-parity assignments and the half-life of the 1376 keV level are taken from Ref. [15]. Parentheses indicate the ranges of possible spin values assuming that the observed transitions have multipolarities of order one or two. Level energies were obtained by fitting the γ-ray energies to the level scheme using the least-squares method [24].

known level and then steps from (a) to (e) were repeated for higher levels.

A. Level scheme of ^{42}K

In the present work 43 transitions were observed in coincidence with ^{42}K recoil nuclei, 22 of which were previously unknown (see Table II). Seven of these new transitions were also seen in the proton-γ and γ-γ coincidence spectra. The 1044 and 1612 keV transitions cited by Warburton *et al.* [13] were confirmed. These transitions were not included in the last compilation of experimental data of ^{42}K [15], because the authors were not sure about their assignment to this nucleus due to low statistics (1044 keV) and contaminants (1612 keV).

Applying the procedure described before, eight new excited states were determined. The level scheme proposed in this work is shown in Fig. 7, where the new levels are marked with asterisks. The existence of the 2992 and 3560 keV levels agrees with the suggestion of Warburton *et al.* [13], and in this work a 633 keV transition is placed as a new branch in the decay of the 2992 keV level besides the 1044 keV transition. Six transitions (542, 736, 1291, 1297, 1511, and 1920 keV) could not be included in the level scheme using the developed procedure. In the work of Krusche *et al.* [12] one finds a 735.1 keV transition between the 842 and 107 keV levels. This assignment was discarded for the 735.7 keV transition, because it did not satisfy the χ^2 condition, and the 735.7 keV γ ray was not measured in coincidence with the 107 keV γ-ray transition (see Table III).

B. Level scheme of ^{43}K

The γ-ray spectrum in coincidence with ^{43}K nuclei revealed 33 transitions, 16 of which were observed originally (see Table IV). The new transition with 1816 keV was present also in coincidence with protons and with 1112 keV γ rays. Figure 8 shows the ^{43}K level scheme proposed in this work.

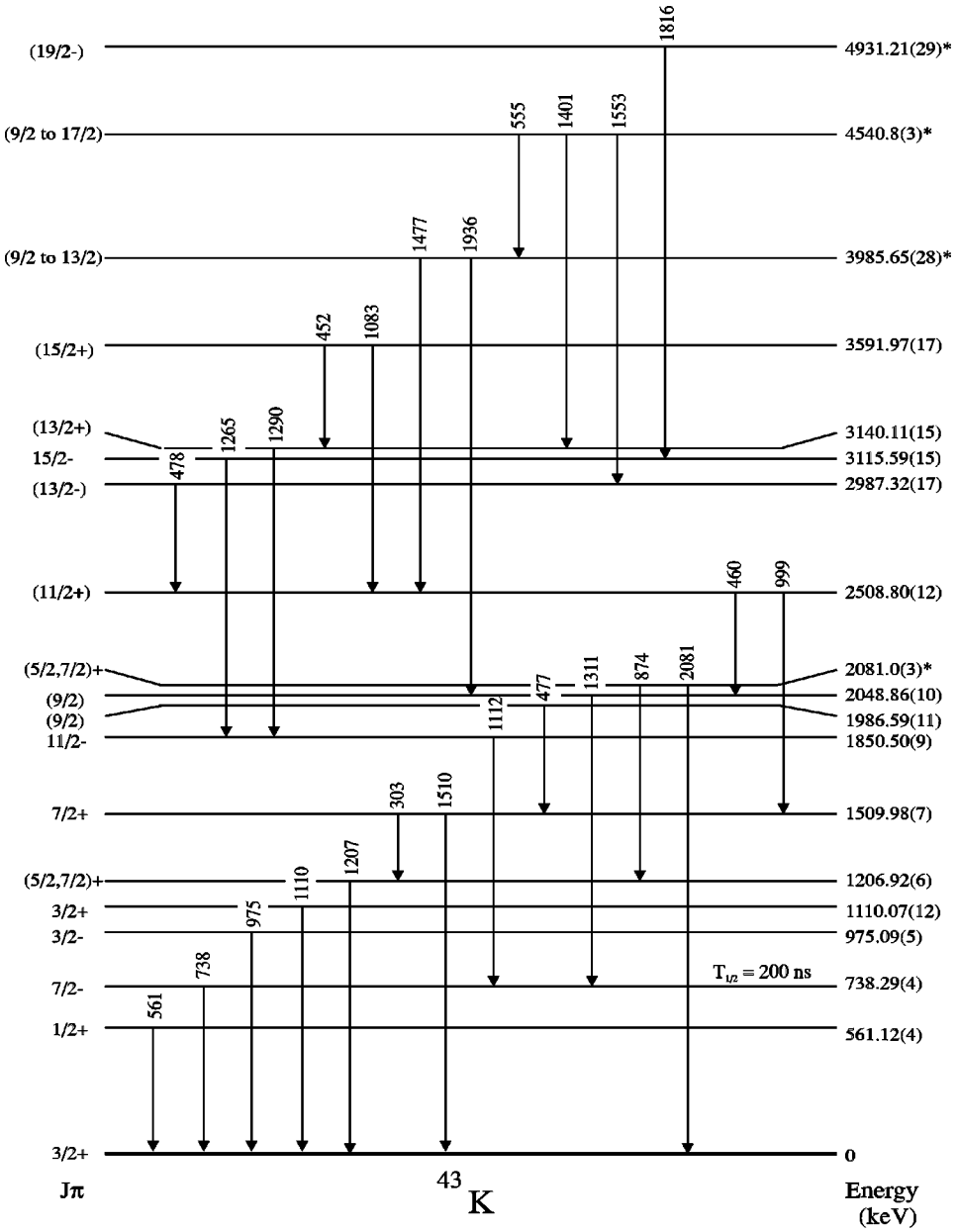

FIG. 8. Level scheme of ^{43}K proposed in this work (see also caption of Fig. 7).

Recently, Kozub *et al.* [17] measured proton-gated γ-ray spectra of the reaction ^{36}S $+^{9}$Be, and reported γ rays belonging to ^{43}K that were not known until the last review of Endt [15]. In the present work the same reaction of Kozub *et al.* was used and the 452, 478, and 1083 keV transitions were confirmed. Furthermore, eight additional transitions supported the suggestion of four levels, with energies of 2081, 3986, 4541, and 4931 keV. The first of them is probably the previously reported level with 2086 ± 10 keV and spin-parity assignment of $J^{\pi}=5/2^{+}$ or $7/2^{+}$ [15]. Three transitions with 414, 549, and 631 keV cited in Ref. [17] were not observed in this work. The 414 and 631 keV are probably too weak, and the 549 keV transitions was not resolved from a 548 keV transition produced in the Coulomb excitation of the gold backing.

The inclusion of the 4931 keV level followed a different criterion. The 1816 keV transition has high intensity and is probably responsible for the decay of an yrast state, but it did not satisfy the necessary conditions of our procedure to determine a new level. It was observed in coincidence with the 1112 keV transition, but does not need to feed the 1850 keV level, otherwise it would be observed in previous experiments. The only level above 1850 keV that can be fed with its intensity is the one with 3116 keV, which decays through the 1265 keV γ ray. The 1265–1816 keV γ-ray coincidence was not observed due to low statistics. A comparison with negative-parity levels of ^{45}Sc (see the next section) suggests that this transition corresponds to the decay of a $J^{\pi}=19/2^{-}$ level at 4931 keV to the 3116 keV level with $J^{\pi}=15/2^{-}$.

IV. INTERPRETATION

Results of shell-model calculations for both ^{42}K and ^{43}K were reported by Johnstone [25]. The author used the $(d_{3/2}s_{1/2})^{-1}(f_{7/2})^{n}$ and $(d_{3/2})^{-1}(f_{7/2})^{n-1}(p_{3/2})$ configurations $(n=A-39)$ to obtain states with $J^{\pi}=0^{-}$ to 5^{-} for ^{42}K and $J^{\pi}=1/2^{+}$ to $19/2^{+}$ for ^{43}K. The most recent calculations for ^{42}K, performed by Retamosa *et al.* [26], show results which are similar to those of Johnstone [25]. Negative and positive-parity states of ^{42}K were also calculated by Hasper (cited in

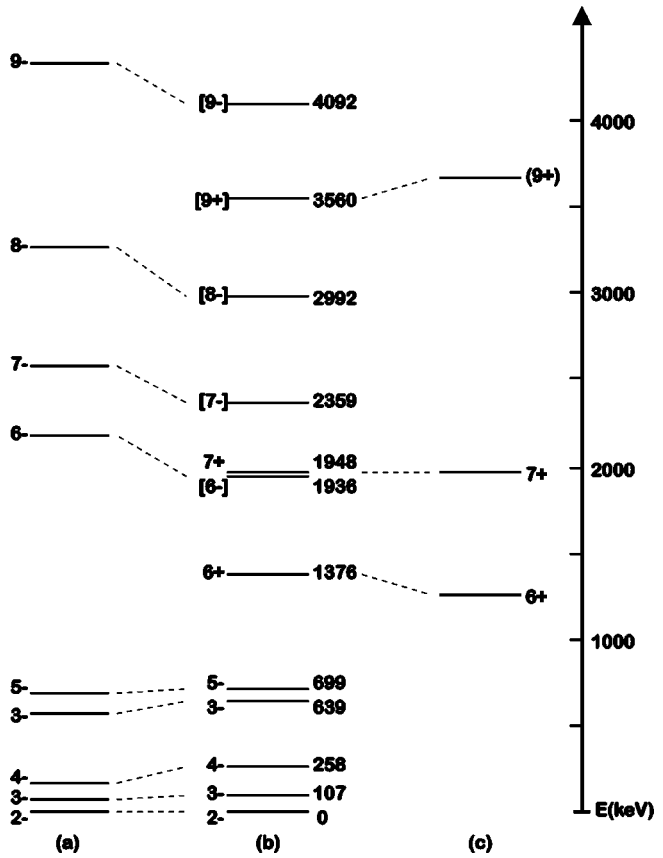

FIG. 9. Comparison between levels of ^{42}K obtained in shell-model calculation (a), experiment (b), and weak-coupling approximation using ^{44}Sc (c). The shell-model energies were normalized relative to the ground state. The center of mass of the three levels of ^{44}Sc [8] was chosen the same as the center of mass of the corresponding levels of ^{42}K. Spins and parities in square brackets should be read as suggestions and not as assignments.

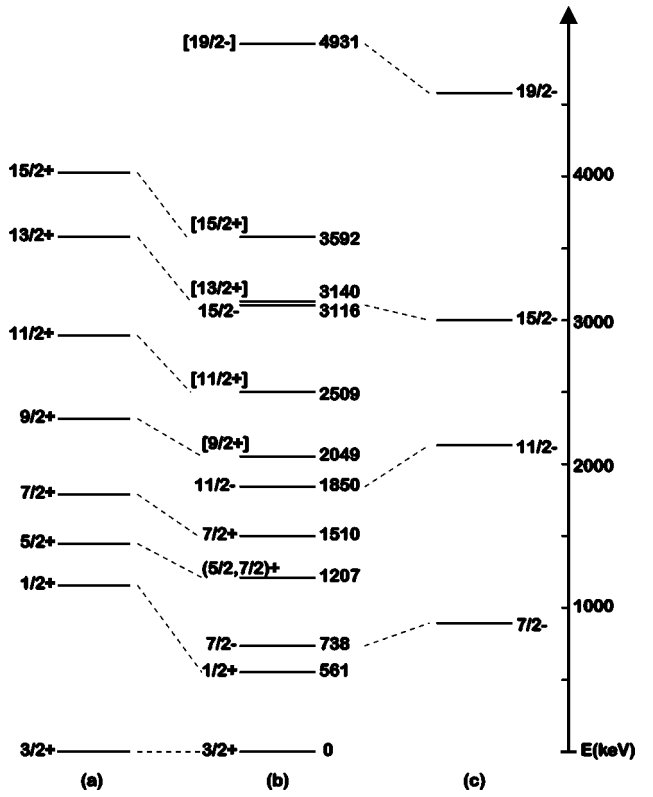

FIG. 10. Comparison between levels of ^{43}K obtained in shell-model calculation (a), experiment (b), and weak coupling approximation using ^{45}Sc (c). The center of mass of the four levels of ^{45}Sc [15] was chosen the same as the center of mass of the corresponding levels of ^{43}K (see also caption of Fig. 9).

the work of Ekström [14]), using the $(d_{3/2})^{n_1}(f_{7/2})^{n_2}(p_{3/2})^{n_3}$ space with $n_1 \geq 4$, $n_2 \leq 4$, and $n_3 \leq 2$. The interpretation of several levels was possible based on the results cited above, but they are very restricted in energy and angular momentum.

The γ-ray spectrum in coincidence with ^{42}Ca, which was produced in the strongest channel, revealed transitions from levels with reliable spin assignment of $9\hbar$, like the 6554 keV level, and from levels with uncertain spin assignments up to $11\hbar$, like the 7751 and 8297 keV levels [15]. Excited levels with such spins were probably populated also in the potassium isotopes. Although the results of our experiments did not permit a determination of spins and parities, we have attempted to interpret some of the observed levels by using two approaches. The first one consisted of shell-model calculations in the $(sd)^{-1}(fp)^n$ space to obtain negative- (positive-) parity levels of ^{42}K (^{43}K) with $n=3$ ($n=4$). The interactions used in the calculations were the same as described in [27]. The opposite parity levels were interpreted with the weak-coupling approximation, because the sizes of the matrices for $(sd)^{-2}(fp)^{n+1}$ calculations would be prohibitively large and truncation could produce spurious configurations. This approximation was performed by utilizing known levels of scandium isotopes, which have the $Z=20$ closed shell plus one proton in the fp shell. Considering that 18 protons of the potassium isotopes couple to $J^\pi = 0^+$ and the valence proton occupies the fp shell, the weak-coupling approximation is carried out by comparing levels of $^{44}_{21}\mathrm{Sc}_{23}$ and $^{45}_{21}\mathrm{Sc}_{24}$ with levels of $^{42}_{19}\mathrm{K}_{23}$ and $^{43}_{19}\mathrm{K}_{24}$, respectively.

A. ^{42}K

The negative-parity levels of ^{42}K predicted by the shell-model calculations are shown in the left part of Fig. 9. The order of the lower levels with $J^\pi = 2^-, 3^-, 4^-, 3^-$, and 5^- is well reproduced and the general agreement of the energies is good. The main configuration of this lowest multiplet consists of three neutrons in the fp shell coupled to $7/2^-$ (as in the ^{43}Ca ground state) plus a proton hole in the $d_{3/2}$ orbital. The main configuration of the 9^- level consists of three neutrons in the fp shell coupled to $15/2^-$ (as in the ^{43}Ca state at 2.74 MeV) plus a proton hole in the $d_{3/2}$ orbital. The calculated spectrum for the negative-parity yrast states in ^{42}K is more spread out than that of the yrast states in ^{43}Ca, indicating a collective structure to these states beyond that expected from a pure weak-coupling model. The shell-model results for the energies of the $J^\pi = 6^-, 7^-, 8^-$, and 9^- levels are systematically higher than the corresponding experimental levels shown in the central portion of Fig. 9. This systematic shift of the shell-model levels is also present in the predictions of Warburton and Becker [28] for ^{40}Cl, as shown in the work of Balamuth *et al.* [9], and for levels of ^{43}K, as will be

shown below. This systematic shift in all of these nuclei probably indicates that the particle-hole strength of the interaction described in [27] needs to be adjusted, or it may mean that the collectivity of these states is larger than can be obtained within the present model space.

The positive-parity levels with $E=1143$, 1376, 1539, and 1948 keV have been previously interpreted in the work of Ekström *et al.* [14] as having $J^{\pi}=4^{+}$, 6^{+}, 5^{+}, and 7^{+}, respectively. The 6^{+}, 7^{+}, and 9^{+} levels of ^{44}Sc reported by Kolata *et al.* [8] are shown in the right part of Fig. 9. A great similarity is observed between the relative energies of the 6^{+} and 7^{+} levels of ^{42}K and ^{44}Sc. This similarity suggests an assignment of $J^{\pi}=9^{+}$ for the 3560 keV level.

B. ^{43}K

The positive-parity levels calculated with the shell model for ^{43}K are presented in the left part of Fig. 10. Like for the case of ^{42}K, the calculated energies are higher than the experimental ones. The similarities of some negative-parity states of ^{43}K and ^{45}Sc have been noticed previously by Behbehani *et al.* [16], which compared the levels of both nuclides with angular momenta up to $15\hbar/2$. The corresponding levels of ^{45}Sc are shown in the right part of Fig. 10, which was the basis for the suggestion of the 4931 keV $J^{\pi}=19/2^{-}$ level. Although there is no previous evidence of this level, its existence has been speculated earlier by Kozub *et al.* [17].

V. CONCLUSION

The information about the γ-ray spectra of ^{42}K and ^{43}K has been substantially improved with the results of the present work. Several transitions of both isotopes were observed, which permitted the suggestion of several new levels. The employment of recoil-nuclei-γ spectroscopy was of great importance for the unique identification of the new transitions.

Part of the level schemes of both nuclides were interpreted by using the shell model with the $(sd)^{-1}(fp)^{n}$ model space. Systematic discrepancies between calculated and experimental levels indicate that the particle-hole interaction is too large, or that the model space is not sufficient to describe the collectivity of the actual levels.

ACKNOWLEDGMENTS

We would like to acknowledge the group of Professor J. de Boer for providing the four HPGe detectors used in the second experiment, and Dr. Dirk Rudolph for valuable discussions. This work was partially supported by CAPES (Coordenação de Aperfeiçoamento de Pessoal de Nível Superior) Brazil, CNPq (Conselho Nacional de Desenvolvimento Científico e Tecnológico) Brazil, FAPESP (Fundação de Amparo à Pesquisa do Estado de São Paulo) Brazil, and BMBF (Bundesministerium für Bildung, Wissenschaft, Forschung und Technologie) Germany. B.A.B. acknowledges support from NSF Grant No. PHY-9605207.

[1] R.W. Bauer, A.M. Bernstein, G. Heymann, E.P. Lippincott, and N.S. Wall, Phys. Lett. **14**, 129 (1965).
[2] W.J. Gerace and A.M. Green, Nucl. Phys. **A93**, 110 (1967).
[3] C.W. Towsley, D. Cline, and R.N. Horoshko, Nucl. Phys. **A204**, 574 (1973).
[4] P. Betz, E. Bitterwolf, B. Busshardt, and H. Röpke, Z. Phys. A **276**, 295 (1976).
[5] A.H. Behbehani *et al.*, J. Phys. G **5**, 1117 (1979).
[6] Th. Kern, P. Betz, E. Bitterwolf, F. Glatz, and H. Röpke, Z. Phys. A **294**, 51 (1980).
[7] E. Bitterwolf *et al.*, Z. Phys. A **313**, 123 (1983).
[8] J.J. Kolata, J.W. Olness, and E.K. Warburton, Phys. Rev. C **10**, 1663 (1974).
[9] D.P. Balamuth, U.J. Hüttmeier, and J.W. Arrison, Phys. Rev. C **48**, 2648 (1993).
[10] J.A. Cameron *et al.*, Phys. Rev. C **49**, 1347 (1994).
[11] S.M. Lenzi *et al.*, Z. Phys. A **354**, 117 (1996).
[12] B. Krusche *et al.*, Nucl. Phys. **A439**, 219 (1985).
[13] E.K. Warburton, J.J. Kolata, and J.W. Olness, Phys. Rev. C **11**, 700 (1975).
[14] L.P. Ekström, H.H. Eggenhuisen, G.A.P. Engelbertink, J.A.J. Hermans, and H.J.M. Aarts, Nucl. Phys. **A283**, 157 (1977).
[15] P.M. Endt, Nucl. Phys. **A521**, 1 (1990).
[16] A.H. Behbehani, A.M. Al-Naser, L.L. Green, A.N. James, C.J. Lister, N.R.F. Rammo, J.F. Sharpey Shafer, H.M. Sheppard, and P.J. Nolan, J. Phys. G **5**, 971 (1979).
[17] R.L. Kozub *et al.*, Phys. Rev. C **46**, 1671 (1992).
[18] F. Pühlhöfer, Nucl. Phys. **A280**, 267 (1977).
[19] K. Rudolph, D. Evers, P. Konrad, K.E.G. Löbner, U. Quade, S.J. Skorka, and I. Weidl, Nucl. Instrum. Methods Phys. Res. **204**, 407 (1983).
[20] K.E.G. Löbner, U. Lenz, U. Quade, K. Rudolph, W. Schomburg, S.J. Skorka, and M. Steinmayer, Nucl. Instrum. Methods Phys. Res. B **26**, 301 (1987).
[21] T.W. Burrows, Nucl. Data Sheets **48**, 1 (1986).
[22] L.K. Pecker, Nucl. Data Sheets **68**, 271 (1993).
[23] R.G. Helmer and A. Bäcklin, Nucl. Instrum. Methods **65**, 31 (1968).
[24] V.R. Vanin, G. Kenchian, M. Moralles, O. Helene, and P.R. Pascholati, Nucl. Instrum. Methods Phys. Res. A **391**, 338 (1997).
[25] I.P. Johnstone, Phys. Rev. C **22**, 2561 (1980).
[26] J. Retamosa, E. Caurier, F. Nowacki, and A. Poves, Phys. Rev. C **55**, 1266 (1997).
[27] H. Scheit *et al.*, Phys. Rev. Lett. **77**, 3967 (1996).
[28] E.K. Warburton and J.A. Becker, Phys. Rev. C **39**, 1535 (1989).